

Quantitative Phase Imaging Using Hard X Rays

K. A. Nugent,¹ T. E. Gureyev,^{1,*} D. F. Cookson,² D. Paganin,¹ and Z. Barnea¹

¹*School of Physics, The University of Melbourne, Parkville, Vic. 3052, Australia*

²*Australian Nuclear Science and Technology Organization, Private Mail Bag 1, Menai, NSW, 2234, Australia*

(Received 22 April 1996)

The quantitative imaging of a phase object using 16 keV x rays is reported. The theoretical basis of the techniques is presented along with its implementation using a synchrotron x-ray source. We find that our phase image is in quantitative agreement with independent measurements of the object. [S0031-9007(96)01227-6]

PACS numbers: 07.85.Qe, 41.50.+h, 42.30.Rx, 42.30.Yc

X-ray imaging is a subject of wide international interest because of the high penetrability and short wavelength of x rays. However, as the energy of the radiation increases, the image contrast due to absorption diminishes. By comparison, the phase shift, if it can be rendered visible, remains relatively high. For example, for 10 Å radiation, approximately 3 μm of carbon produces a 2π phase shift and 50% absorption. If the wavelength is decreased to 1 Å, 3 mm of carbon is required to produce 50% absorption while only 30 μm is required to produce a 2π phase shift. Thus, for imaging with hard x rays there is a considerable premium on being able to use phase as the contrast mechanism.

We define *phase-contrast imaging* as any technique that renders phase variations visible. In the optical region, this includes both Nomarski and schlieren techniques. We propose that the term *phase imaging* be limited to techniques that are able to produce an image in which the contrast is proportional to the phase shift. Zernike phase-contrast imaging falls into this category when the phase shifts are small. We define *quantitative phase imaging* as techniques that yield quantitative phase images of the object. To date, in the x-ray region, quantitative phase imaging is only possible via interferometric techniques; the temporal and spatial coherence requirements therefore place severe constraints on the source. In this paper, we describe a noninterferometric quantitative phase-imaging technique.

Phase-contrast techniques, as defined in the previous paragraph, have been presented in a number of earlier papers. Differential phase contrast using crystal diffraction was first demonstrated by Forster, Goetz, and Zaumseil [1]; these authors described their technique as an x-ray schlieren method. Related work has been published by Somenkov, Tkalic, and Shil'stein [2]; Ingal and Beliaevskaya [3]; Davis *et al.* [4,5]; Gao, Davis, and Wilkins [6]; and Cloetens *et al.* [7]. All of these approaches provide differential phase contrast, or schlieren, imaging that relies on the deviation of the radiation as it encounters phase gradients. Snigirev *et al.* [8,9] have also recently performed some work on phase-contrast imaging that has a close relationship to that presented here, and this technique may be shown to yield a map

of the Laplacian of the phase distribution. In the very soft x-ray region, Schmahl and co-workers have published [10,11] phase-imaging work that is a direct analog of Zernike phase contrast microscopy. Momose, Takeda, and Itai [12] have recently published a phase-imaging technique based on an x-ray interferometer.

In this Letter we develop quantitative phase imaging using the so-called transport of intensity equation [13] that relates the propagation of the intensity distribution to the phase distribution in a wave in the paraxial approximation. Much work has recently been published on the solution of this equation, particularly in the context of adaptive optics in the visible region [14–16]. Gureyev and Nugent [17] have recently shown how the transport of intensity equation may be solved without explicitly seeking the boundary conditions for the solution. It is this theoretical work that we develop and implement experimentally in the current paper.

Consider a scalar paraxial monochromatic wave

$$u(x, y, z) = I^{1/2}(x, y, z) \exp\{ikz + i\varphi(x, y, z)\} \quad (1)$$

with intensity $I(x, y, z)$, slowly varying phase $\varphi(x, y, z)$, and $k = 2\pi/\lambda$. If the intensity is nonzero everywhere in an open region Ω of the plane $z = z_0$, then, in Ω , the intensity and phase satisfy the transport of intensity equation (TIE):

$$k \frac{\partial I}{\partial z} = -\nabla \cdot (I \nabla \varphi). \quad (2)$$

If the intensity $I(x, y, z_0)$ is equal to zero both at the boundary and outside Ω , then the TIE, Eq. (2), has a phase solution which is unique up to an arbitrary additive constant [18].

We consider a method for finding the solution to the TIE in a rectangular region $\Omega_{ab} = (0, a) \times (0, b)$. We introduce the Fourier harmonics W_{mn} and the standard scalar product $\langle f, g \rangle$ in Ω_{ab} :

$$W_{mn}(x, y) = \exp\{i2\pi mx/a\} \exp\{i2\pi ny/b\}, \quad (3)$$

$$\langle f, g \rangle = \frac{1}{ab} \int_0^b \int_0^a f(x, y) g^*(x, y) dx dy. \quad (4)$$

The Fourier harmonics are orthonormal with respect to this scalar product. Let the intensity derivative be approximated by a finite sum of Fourier harmonics,

$$k \frac{\partial I}{\partial z} = \sum_{m,n} F_{mn} W_{mn}, \quad |m| \leq M, \quad |n| \leq N. \quad (5)$$

We seek a phase of similar form,

$$\varphi = \sum_{m,n} \varphi_{mn} W_{mn}, \quad |m| \leq M, \quad |n| \leq N. \quad (6)$$

To find this phase we take the scalar product (4) of Eq. (2) and a Fourier harmonic W_{pq} , integrate by parts using the fact that the boundary integral vanishes, as $I = 0$ at the boundary, and obtain $\langle I \nabla \varphi, \nabla W_{pq} \rangle = F_{pq}$. Substituting the representation Eq. (6), we arrive at the following system of algebraic equations for the unknown Fourier coefficients of the phase:

$$\sum_{m,n} L_{pq}^{mn} \varphi_{mn} = ab F_{pq}, \quad (7)$$

$$L_{pq}^{mn} = (2\pi)^2 (mpb/a + nqa/b) I_{(p-m)(q-n)}, \quad (8)$$

where $|m|, |p| \leq M$ and $|n|, |q| \leq N$, and $I_{mn} = \langle I, W_{mn} \rangle$ are the Fourier coefficients of the intensity distribution $I(x, y, z = 0)$.

This system of equations may be solved in general, and this will be reported in a further publication. For the purposes of this Letter, however, let us consider the special case of a uniform intensity distribution such that $I(x, y, 0) \equiv I_0$ in Ω_{ab} and $I(x, y, 0) \equiv 0$ both outside Ω_{ab} and at the boundary. Clearly, in this case, I_{mn} is only nonzero when $p = m$ and $q = n$ so that the Fourier coefficients of the phase reduce to

$$\varphi_{mn} = \frac{(ab)^2}{(2\pi)^2 (m^2 b^2 + n^2 a^2) I_0} F_{mn}, \quad (9)$$

with the range of indices defined following Eq. (8) but where $m^2 + n^2 \neq 0$. Thus, in order to calculate the phase from the z derivative of the intensity in the case of uniform illumination, it is sufficient to perform the Fourier transform of $k \partial I / \partial z$, reweight its Fourier coefficients in accordance with (9), and perform the inverse Fourier transform.

We are thus led to a very rapid approach to the recovery of the phase from intensity with the unusual benefit that no separate determination of boundary conditions is required. A full discussion of this theoretical approach will be presented in a future paper. In the present paper we present the results of an experiment in which these ideas are tested using hard x rays.

The experiment sketched in Fig. 1 was assembled at beam line 20 A (Australian National Beamline Facility) at the Photon Factory synchrotron at KEK in Tsukuba, Japan. The monochromator was adjusted so as to produce a beam of 16 keV x rays. The resulting x-ray beam has a divergence of approximately 0.38 mrad in the horizontal and 0.037 mrad in the vertical. Two 100 μm square apertures were placed in the beam to produce a highly

uniform beam with a square profile. The prime purpose of the apertures is to limit the effective source size in the synchrotron and thus produce enhanced spatial coherence in the x-ray beam. Smaller apertures were not used as the effect we seek is effectively the redirection, through refractive index variations in the object, of optical energy from one point in the detection plane to another; this clearly requires that a significant amount of the object be illuminated at any one time.

A commercial carbon electron microscope calibration grid (SPI model 411CG-AB) with a period of 330 μm was used as our test object. It was placed in an approximately square Pb defining aperture. The x-ray optical thickness of the grid was measured by observing the absorption of 8.05 keV x rays through the grid. The grid was measured to have an average effective thickness of $68 \pm 24 \mu\text{m}$ of solid density carbon. The uncertainties arise partially from genuine variations in the grid thickness but primarily from a poor signal to noise ratio in the absorption measurement due to the low absorption of the grid at this energy.

Our phase-imaging experiments were performed with an x-ray energy of 16 keV for which maximum absorption by the object is about 0.7%. Our experimental arrangement did not allow us to measure the absorption image of the object immediately behind the object for 16 keV x rays, and so we were precluded from directly observing the absorption of 16 keV x rays. However, we took absorption to be negligible in our experiment.

A 15×15 micron pinhole was placed in front of an Ar filled ion chamber 1.68 m from the object. The object was scanned in 20 μm steps and the signal was integrated for approximately 1 sec at each point of the scan. The resulting image showed contrast resulting from the refractive effects in the carbon grid. The resulting data are shown in Fig. 2 after they have been cropped to a square shape and where the large constant background has been subtracted; this is effectively the value of $\partial I / \partial z$ and is therefore the direct input to our reconstruction algorithm. These data were Fourier transformed using a fast Fourier transform (FFT) algorithm and the resulting spectrum multiplied by a filter of the form given in Eq. (9).

Two important steps were taken in preparation of the data for analysis: First, since the intensity distribution at the object plane was not measured, the input data we use for $\partial I / \partial z$ might be in error by an additive constant due to divergence in the incident radiation. Second, in preparation for processing using the FFT, our data

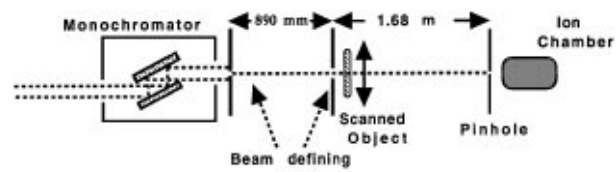


FIG. 1. Schematic of the experimental arrangement.

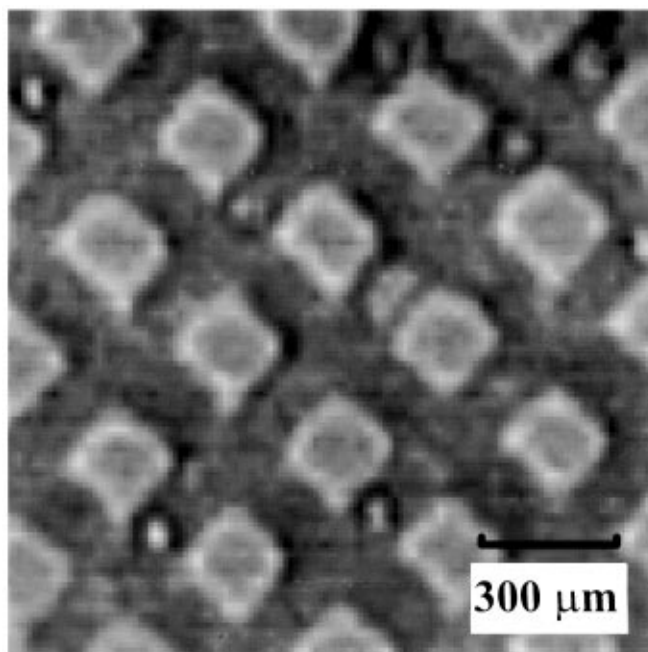


FIG. 2. Experimental data with the large constant background subtracted. The contrast on the data before background subtraction was approximately 7%.

were cropped to a square format which precluded the direct measurement of the edge effects in the data. The consequence of the first step is the loss of any information on the divergence in the incident field. The consequence of the second is the loss of information at the boundary.

Loss of information on the divergence of the field will be manifest as the presence of the Z_4 Zernike polynomial in a Zernike decomposition of the phase image [16]. The removal of the boundary signal is equivalent to the addition of some linear combination of “diagonal” Zernike polynomials to the phase image where the diagonal Zernike polynomials represent the class of phase variations that are manifest only at the boundary in this form of experiment [16]. To eliminate these components we perform a Zernike decomposition of the phase image and subtract the low-order diagonal components and the Z_4 component. The practical effect of this subtraction is to eliminate the slowly varying background indirectly produced by the preparation of our data for analysis. This approach was very successful, and the resulting image is shown in Fig. 3; note that the Zernike decomposition is most conveniently performed on a circular set of data. Prior to this subtraction, the low-order components obscured much of the image information.

The apertures used in the experiment limited the effective source shape to a well-defined square. It is straightforward to show that the resulting phase image is the true phase image convolved with the square source distribution. In principle, then, the image could be corrected by deconvolving out the effect of the source using standard Fourier techniques. However, this course

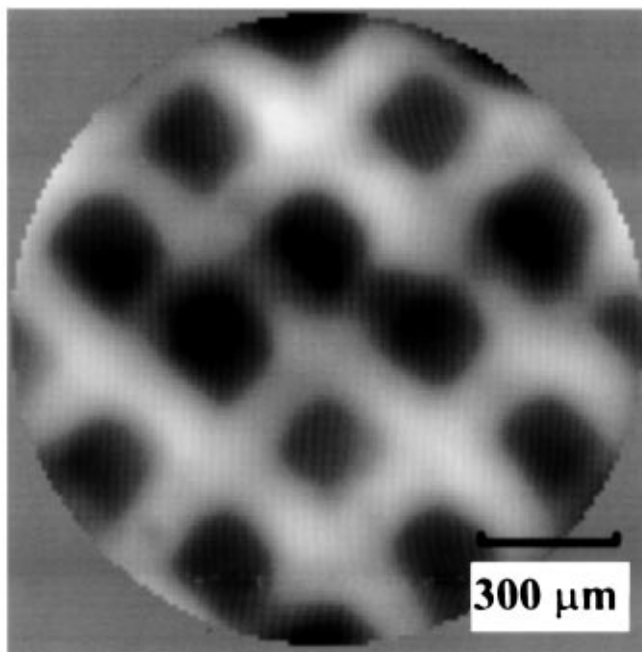


FIG. 3. Direct reconstruction of the experimental data.

would inevitably lead to noise amplification around the zeros in the reconstructing filter. In order to eliminate this problem and to take a very conservative approach to image reconstruction, we used a modified filter that approximately compensated for the source blurring.

The blurring due to a square source may be compensated by multiplying the Fourier components of the image by $F(k) = ak/\sin(ak)$, where $2a$ is the source width. In our data, we used a deblurring filter of the form

$$F'(k) = \begin{cases} \frac{1}{1 - \frac{4}{27}(ak)^2} & |k| \leq \frac{3}{2a} \\ |ak| & |k| > \frac{3}{2a} \end{cases}. \quad (10)$$

This filter always amplifies the spatial frequencies less than or equal to the amount required by the full deconvolution filter $F(k)$ [i.e., $|F'(k)| \leq |F(k)| \forall k$] and is a smooth function that very closely mimics the true filter to second order for $|k| \leq 3/2a$.

The effective source size $2a$ in our experiment was directly determined by scanning an edge through the experimental setup. The modified full reconstruction filter is shown in Fig. 4. It can be seen that the suppression of frequencies is much less than for the unmodified filter but that no frequencies are amplified; the result is that the reconstruction is sharper while remaining rather insensitive to noise contamination. The image after the application of the modified filter is shown in Fig. 5, and it can be seen to be much sharper when compared with the previous image.

As reported earlier, we measured the x-ray optical thickness of the object using 8 keV x-ray absorption. This measurement allows us to predict the phase shift

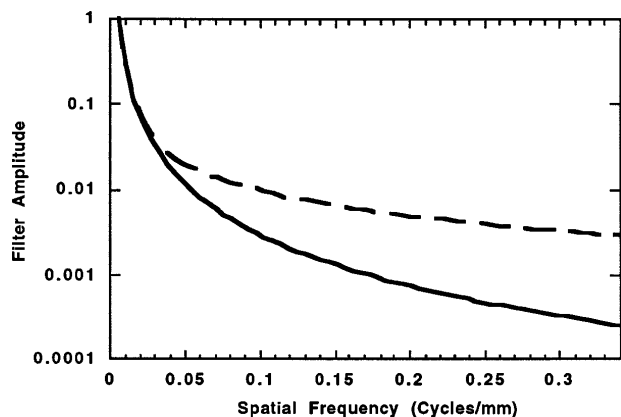


FIG. 4. Filters used in the reconstruction. The dashed line indicates the theoretical phase retrieval filter. The solid line indicates the modified filter that partially compensates for the finite source size. Note that there is no frequency amplification in either of these filters.

for 16 keV x rays using the known complex atomic scattering factors for carbon. Using this approach, the average phase shift of the grid bars for the 16 keV x rays was predicted to be $(2.9 \pm 1.0)\pi$. Our phase image produced an average phase shift of $(3.3 \pm 0.3)\pi$, in good agreement with the deduction obtained via our absorption measurement. We thus conclude that we have indeed managed to quantitatively recover the phase distribution of the x rays. Note that use of the deblurring filter described in the previous paragraph merely sharpens the resulting image; it does not affect the thickness deduced from the phase image.

In conclusion, then, we have presented the theoretical basis for, and an experimental confirmation of, quantitative noninterferometric phase imaging using 16 keV

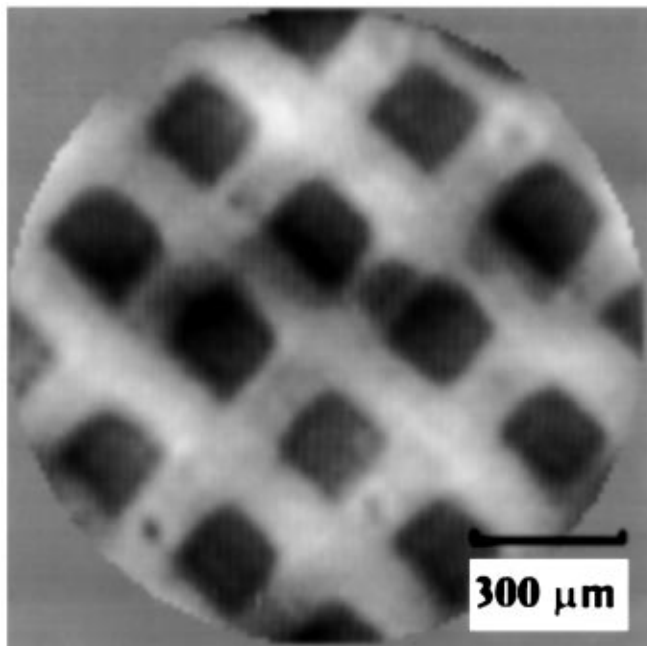


FIG. 5. Phase image obtained with the modified filter.

x rays. The experimental arrangement is extremely simple, and our phase imaging implies a phase shift for the test object that is in quantitative agreement with that deduced from an independent absorption measurement. We take the agreement between our measured phase shift and the simple absorption-based deduction as experimental confirmation that our phase images are indeed quantitatively correct.

This work was supported by grants from the Australian National Beamline Facility, a consortium of Australian universities, ANSTO, DIST, and the Australian Research Council. D.P. acknowledges the receipt of an Australian Postgraduate Award. The authors acknowledge valuable conversations with David Balaic and Andrew Peele during the course of this work.

*Also with CSIRO Division of Forestry and Forest Products, Private Bag 10 Clayton, Vic, 3169, Australia.

- [1] E. Forster, K. Goetz, and P. Zaumseil, *Kris. Tech.* **15**, 937–945 (1980).
- [2] V. A. Somenkov, A. K. Tklich, and S. Sh. Shil'stein, *Sov. Phys. Tech. Phys.* **36**, 1309–1311 (1991).
- [3] V. N. Ingal and E. A. Beliaevskaya, *J. Phys. D* **28**, 2314–2317 (1995).
- [4] T. J. Davis, D. Gao, T. E. Gureyev, A. W. Stevenson, and S. W. Wilkins, *Nature (London)* **373**, 595–598 (1995).
- [5] T. J. Davis, T. E. Gureyev, D. Gao, A. W. Stevenson, and S. W. Wilkins, *Phys. Rev. Lett.* **74**, 3173–3176 (1995).
- [6] D. Gao, T. J. Davis, and S. W. Wilkins, *Aust. J. Phys.* **48**, 103–111 (1995).
- [7] P. Cloetens, R. Barrett, J. Baruchel, J-P. Guigay, and M. Schlenker, *J. Phys. D* **29**, 133–146 (1996).
- [8] A. Snigirev, I. Snigireva, V. G. Kohn, S. Kuznetsov, and I. Schelokov, *Rev. Sci. Instrum.* **66**, 5486–5492 (1995).
- [9] A. Snigirev, I. Snigireva, V. G. Kohn, and S. M. Kuznetsov, *Nucl. Instrum. Methods Res., Sect. A* **370**, 634–640 (1995).
- [10] G. Schmahl, D. Rudolph, and P. Guttmann, in *Phase Contrast X-ray Microscopy Experiments at the BESSY Storage Ring*, edited by D. Sayre, M. Howells, J. Kirz, and H. Rarback, *X-Ray Microscopy II* (Springer-Verlag, Berlin, 1987), pp. 228–232.
- [11] G. Schmahl, P. Guttmann, G. Schneider, B. Niemann, C. David, T. Wilhein, J. Thieme, and D. Rudolph, in *Phase Contrast Studies of Hydrated Specimens with the X-ray Microscope at BESSY*, edited by A. Erko and V. Aristov, *X-Ray Microscopy IV* (Bogorodski Pechatnik, Chernogolovka, Moscow Region, 1994).
- [12] A. Momose, T. Takeda, and Y. Itai, *Rev. Sci. Instrum.* **66**, 1434–1436 (1995).
- [13] M. R. Teague, *J. Opt. Soc. Am.* **73**, 1434–1441 (1983).
- [14] F. Roddier, *Appl. Opt.* **27**, 1223–1225 (1988).
- [15] F. Roddier, *Appl. Opt.* **29**, 1402–1403 (1990).
- [16] T. E. Gureyev, A. Roberts, and K. A. Nugent, *J. Opt. Soc. Am. A* **12**, 1932–1941 (1995).
- [17] T. E. Gureyev and K. A. Nugent, *J. Opt. Soc. Am. A* **13**, 1670–1682 (1996).
- [18] T. E. Gureyev, A. Roberts, and K. A. Nugent, *J. Opt. Soc. Am. A* **12**, 1942–1946 (1995).